Journal of Thermal Analysis, Vol. 38 (1992) 1345-1355

STUDY OF THERMAL DECOMPOSITION OF AMMONIUM CERIUM SULPHATE

I. B. Sharma, V. Singh and M. Lakhanpal*

DEPARTMENT OF CHEMISTRY, UNIVERSITY OF JAMMU, JAMMU – 180 004 INDIA

(Received July 24, 1989; in revised form August 26, 1991)

Thermal decomposition of ammonium cerium sulphate has been studied by differential scanning calorimetry and thermogravimetry. The results show that the material decomposes in five steps in the temperature region 364–1116 K in oxygen. Based on the thermal data, elemental analysis and magnetic susceptibility measurements, sequence of decomposition has been established. The final product has been identified as CeO_2 by X-ray diffractometry. Ammonium cerium sulphate and the products of the first and the final transitions contain cerium ion in 4+ oxidation state, while the three intermediate phases have cerium ion in 3+ oxidation state. From the non-isothermal DSC studies, kinetic parameters have been computed. The isothermal data show that the dehydration process follows Ginstling-Brounshtein mechanism, while the next three steps are governed by Mampel's unimolecular law of random nucleation.

Keywords: ammonium cerium sulphate, DSC, kinetic parameters, TG

Introduction

Thermal investigations of complex compounds are interesting because such studies give understanding of formation of intermediate compounds and mechanism of their formation [1–4]. Some results of thermogravimetric study of ammonium cerium sulphate have also been reported in literature [5]. However, no systematic study seems to have been done on thermal characterization of the material and to understand kinetics of various steps of its decomposition. In the present paper, sequence of thermal decomposition of ammonium cerium sulphate has been studied by thermogravimetry and differential scanning calorimetry.

---

* To whom all correspondence should be addressed.

John Wiley & Sons, Limited, Chichester
Akadémiai Kiadó, Budapest

Kinetic parameters of the processes involved, under dynamic as well as isothermal conditions, have been computed from the differential scanning calorimetric data. Different phases, formed during the thermal treatment, have been characterized by elemental analysis and magnetic susceptibility, while the end product has been identified by X-ray diffractometry.

Experimental

AR grade ammonium cerium(IV) sulphate was used.

Thermal analysis

Thermograms (TG and DSC plots) of the sample were recorded on Mettler thermal analysis system TA 3000, provided with microprocessor TC 10, in continuous flow of nitrogen and oxygen (30 ml/min) separately at a heating rate of 10 deg/min. The thermograms in continuous flow of oxygen are given in Figs 1 and 2. To understand the mechanism of the processes involved, α (fraction of the reaction completed) *vs.* t (time) plots were recorded isothermally on the DSC at three temperatures in the temperature region of the each step. The α *vs.* t plots are given in Figs 3–6.

Elemental analysis

Ammonium cerium sulphate and the phases drawn from the TG cell after runs upto 500.0, 633.4, 721.3, 870 and 1116.0 K, corresponding to completion of the different steps in the thermogravimetric analysis, were analysed for cerium, by usual methods and for nitrogen and hydrogen on a micro-elemental analyzer Carlo Erba Model 1106. The results of the analysis are given in Table 1.

Table 1 Analytical and physical data of the different phases drawn from the TG

Temperature at which the phase is drawn / K	Analysis / %			Molar magnetic susceptibility $\chi_m \cdot 10^6$ / cgs units	μ_{eff} / B.M.
	Ce	N	H		
Ammonium cerium sulphate (unheated)	22.26	8.81	3.11	–6	–
500.0	23.60	9.51	2.65	23	0.235
633.4	26.45	7.83	2.45	1420	1.83
721.3	39.81	3.92	1.14	1345	1.78
870.0	49.60	0.00	0.00	1362	1.80
1116.0	82.61	0.00	0.00	–4	–

Magnetic susceptibility

Room temperature magnetic susceptibility of the samples used for the elemental analysis was recorded on a Gouy magnetic balance at a constant magnetic field of 3000 gauss, using $HgCo(CNS)_4$ as calibrant. The molar magnetic susceptibility of the different samples, after diamagnetic correction for the constituent ions, is given in Table 1.

X-ray diffractometry

Room temperature X-ray diffractograms of the sample, heat-treated at 1116 K, was recorded at a scanning speed of 1 deg/min on a Phillips diffractometer type PW 1050/70 using CuK_α radiations.

Results and discussion

The cerium, nitrogen and hydrogen contents (22.26, 8.81 and 3.11% respectively) of the starting material suggested its stoichiometry as $(NH_4)_4Ce(SO_4)_4$ $2H_2O$. The TG studies in the temperature range 323–1173 K in continuous flow of oxygen (Fig. 1) show that the ammonium cerium sulphate decomposes in five steps. The first step which lies between 364 and 500 K with peak temperature of 438.7 K, is associated with 5.67% mass loss. The second step starts at 573.6 K and is completed at 633.4 K with peak temperature at 623.6 K. The step is associated with 10.3% mass loss. The third step lies between 635 and 721.3 K with peak temperature of 689.3 K and the material loses 30.8% mass in this step. In the fourth step, which lies between 721.3 and 870 K with peak temperature at 782.7 K, the material further loses 11.14% mass. The last step which is associated with 16.90% mass loss, starts at 945.3 K and is completed at 1116 K. Its peak temperature lies at 1086 K.

The TG curve in nitrogen shows that there is slight shift in the temperature regions. The material decomposes in five temperature regions: 368–521.3, 526.7–633, 634–716, 716–812 and 903.301994.7 K with peak temperatures of 430.7, 626, 686.7, 777.3 and 1050 K respectively. The mass loss associated with the different steps is 6.03, 10.50, 31.3, 11.36 and 17% respectively.

DSC studies in oxygen in the temperature range 333–833 K (Fig. 2) show that the decomposition of the material is associated with four endothermic transitions in the temperature regions 393–443, 590–633, 633–715, 723–801.7 K, with peak temperatures of 412.5, 620.7, 704.4, 784.2 K respectively. Enthalpy changes (ΔH) associated with these transitions are given in Table 2.

The magnetic measurements (Table 1) show that ammonium cerium sulphate and the sample drawn from the TG cell after heat-treatment up to 1116 K are diamagnetic while the sample drawn after heat-treatment up to 500, 633.4, 721.3

and 870 are associated with magnetic moment of the order of 0.235, 1.83, 1.78 and 1.81 B.M. respectively. The magnetic moment values suggest that cerium ion in ammonium cerium sulphate and in the samples drawn after heat-treatment at

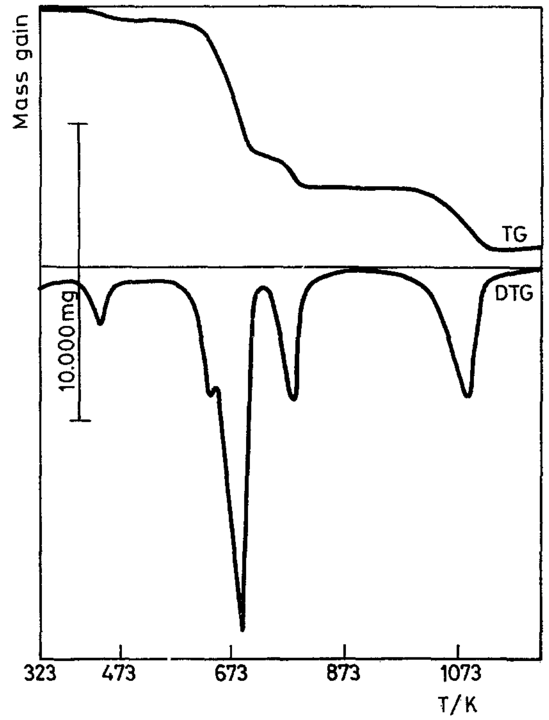

Fig. 1 The TG–DTG curves for ammonium cerium sulphate at the heating rate of 10 deg/min in continuous flow of oxygen (30 ml/min)

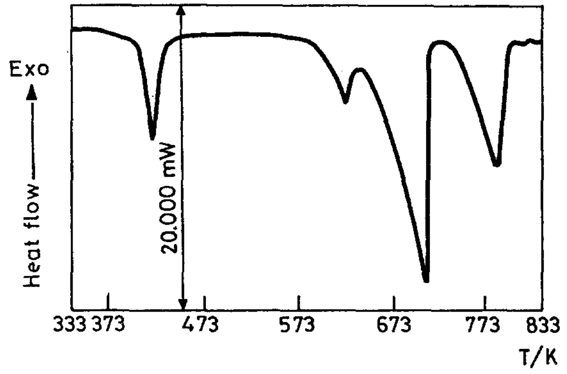

Fig. 2 The DSC curve (dH/dt *vs.* T) for ammonium cerium sulphate at a heating rate of 10 deg/min in continuous flow of oxigen (30 ml/min)

500 and 1116 K is in 4+ oxidation state, while the rest of the intermediate phases contain cerium ion in the 3+ oxidation state. Theoretical value of μ_{eff} for Ce^{3+} is 2.54 BM [6]. However, comparatively lower values of μ_{eff} have been observed. One of the reasons for the low values could be incomplete transformation to the product phase, which is a general tendency of solid state reactions. Formation of CeO_2 as the end product was confirmed by TG weight loss and its characteristic X-ray powder diffraction pattern [7].

Table 2 Kinetic data for thermal decomposition of ammonium cerium sulphate in continuous flow of oxygen with 95% confidence limits in parentheses

Transition temperature / K TG/DSC	Peak temperature / K TG/DSC	E / kJ·mol^{-1}	ln *A*	Δ*H* / J·mol^{-1}	Total mass loss / %*
364 –500 / 393–443	438.7 / 412.5	317 (62.6)	65 (3)	110.31	5.67 (5.70)
573.6–633.4 / 590–633	623.6 / 620.7	284.7 (22.5)	51.4 (4)	90.27	15.97 (15.98)
635 –721.3 / 633–715	689.3 / 704.4	165 (4.4)	40.3 (0.78)	652	46.77 (41.61)
721.3–870 / 623–801.7	782.7 / 784.2	276.2 (9.3)	37.7 (1.47)	369	57.91 (55.05)
995.3–1116	1086				74.81 (72.77)

*Values in the brackets are theoretically calculated.

The thermogravimetric analysis, Differential scanning calorimetry, magnetic susceptibility, elemental analysis and X-ray diffraction data suggest that ammonium cerium sulphate decomposes in continuous flow of oxygen in the following sequence:

$$(NH_4)_4Ce(IV)(SO_4)_4{\cdot}2H_2O \xrightarrow[-2H_2O]{364-500\,K} (NH_4)_4Ce(IV)(SO_4)_4 \qquad (1)$$

$$(NH_4)_4Ce(IV)(SO_4)_4 \xrightarrow[-(2NH_3;\ \frac{1}{2}SO_2+\frac{1}{2}O_2)]{573.6-633.4\,K} (NH_4)_3H{\cdot}Ce(III)(SO_4)_{3.5} \qquad (2)$$

$$(NH_4)_3H{\cdot}Ce(III)(SO_4)_{3.5}$$

$$\xrightarrow[-(2NH_3;\ \frac{3}{2}H_2O;\ \frac{3}{2}SO_2;\ \frac{3}{4}O_2)]{635-721.3\,K} (NH_4)Ce(III)(SO_4)_2 \qquad (3)$$

$$(NH_4)Ce(III)(SO_4)_2 \xrightarrow[-(NH_3;\ \frac{1}{2}SO_2;\ \frac{1}{2}H_2O;\ \frac{1}{4}O_2)]{721.3-870\,K} Ce(III)(SO_4)_{1.5} \tag{4}$$

$$Ce(III)(SO_4)_{1.5} \xrightarrow[-(\frac{3}{2}SO_2;\ -\frac{1}{2}O_2)]{995.3-1116\,K} CeO_2 \tag{5}$$

The transformation of cerium ion from 4+ oxidation state to 3+ state in the intermediate products formed in the second, third and fourth steps is unusual and it seems that the reduction is caused due to evolution of NH_3 in these steps. The observation by Udupa and others [8, 9] that cerium(III) sulphate is stable at high temperature has been confirmed and the studies show that it decomposes between 995.3–1116 K to CeO_2. It has also been observed that change in atmosphere from oxygen to nitrogen does not affect the process.

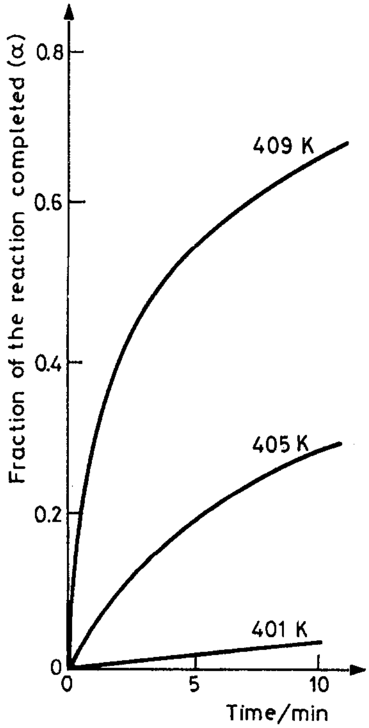

Fig. 3 α *vs.* *t* from the differential scanning calorimetry for the first step of decomposition

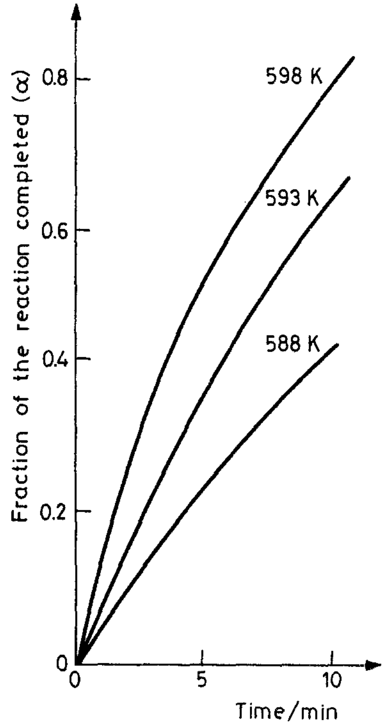

Fig. 4 α *vs.* *t* from the differential scanning calorimetry for the second step of decomposition

Kinetic analysis

Kinetic parameters from the DSC data under dynamic conditions, have been calculated from the relationship [10, 11]:

$$\frac{d\alpha}{dt} = A\, e^{-E/RT}(1-\alpha)^n \tag{6}$$

where α is the fraction of the reaction completed at any time *t*, *E* is the energy of activation, *A* is the pre-exponential factor and *n* is the order of the reaction. Assuming that the fraction of the reaction completed is proportional to the heat taken up or consumed at any instant, the above equation in the logarithmic form is transformed to the following relationship:

$$\ln\frac{dH/dt}{H_t} = \ln A + n\cdot\ln H_r/H_t - \frac{E}{RT} \tag{7}$$

Here, dH/dt, H_t and H_r are the rate of heat flow, total enthalpy change associated with the transition (total peak area) and remaining area of the peak respectively.

From the DSC, dH/dt, H_t, T and H_r are known. Therefore, the other parameters (E, A and n) can be computed.

Based on this principle, E, $\ln A$ and n have been calculated with the aid of a programme available in the microprocessor TC 10, provided with the Mettler thermal analysis system. The kinetic parameters for the different transition steps shown by the DSC plot (Fig. 2) under dynamic conditions are given in Table 2.

The energy of activation (E) and $\ln A$ for the first transition, which is attributed to loss of two water molecules, come out to be 916 kJ/mol and 265 respectively. The high value of $\ln A$ for this step is attributed to highly disordered activated state. Applying Hinshelwood's relation [11]:

$$k=\frac{k_bT}{h}\cdot\frac{(E/RT)^{S-1}}{(S-1)!}\cdot e^{-E/RT} \tag{8}$$

value of S (the number of loose vibrations) has been calculated and comes out to be 13. This suggests that during the loss of water molecules numerous bonds are affected, which implies that the water molecules are structurally co-ordinated.

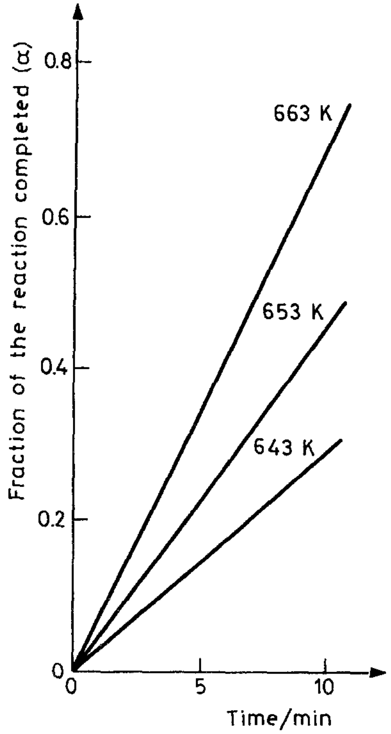

Fig. 5 α *vs.* *t* from the differential scanning calorimetry for the third step of decomposition

Large value of the energy of activation (916 kJ/mole) further substantiates this argument.

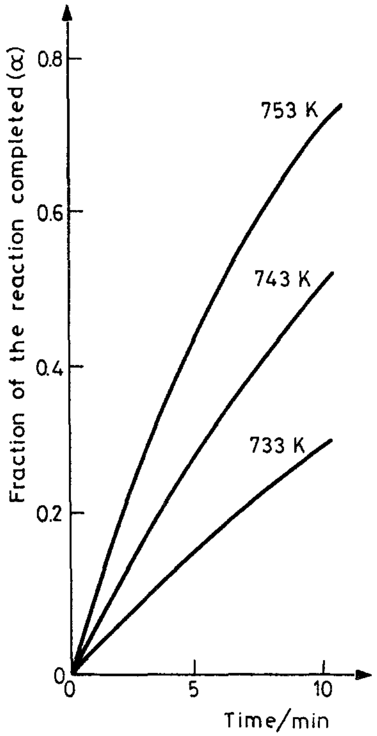

Fig. 6 α *vs*. *t* from the differential scanning calorimetry for the tourth step of decomposition

In the next three steps, where three intermediate products, with 3+ oxidation state, are formed, the values of *S*, as calculated from the Hinshelwood equation, come out equal to 8, 4 and 2 respectively. These values suggest that the decomposition processes in these steps involve lesser number of bonds in each case. Accordingly, energy of activation is also comparatively smaller.

Isothermal data

To understand mechanism of the various steps, different kinetic equations applicable to the solid state reactions, were applied to the isothermal data (Figs 3–6). The data of 401, 405 and 409 K (Fig. 3), corresponding to the loss of two water molecules, follow the Ginstling-Brounshtein equation for the diffusion controlled reactions [12]:

$$kt = 1 - \frac{2}{3}\cdot\alpha - (1-\alpha)^{2/3} \tag{9}$$

Plots of $1 - \frac{2}{3}\cdot\alpha - (1-\alpha)^{2/3}$ *vs.* t are linear. Applicability of Ginstling–Brounshtein equation to the isothermal kinetic data indicated that the diffusion is the rate determining step in the reaction process when the reaction surface of the spherical reactant particles actually decreased in area as the reaction proceeded.

The α *vs.* t data at 588, 593 and 598 K (Fig. 4); 643, 653 and 663 K (Fig. 5); and 733, 743 and 753 K (Fig. 6) follow the Mampel's unimolecular law of random nucleation [13]:

$$kt = -\ln(1-\alpha) \tag{10}$$

Plots of $\ln\ln(1/(1-\alpha))$ *vs.* $\ln t$ are linear in all the cases with slope of the order of unity. The applicability of the Mampel's law suggested that random nucleation of the product phase in spherical microcrystals is the rate determining step in these decomposition steps.

References

1 P. G. Dickens, A. C. Halliwell, D. Murphy and M. S. Whittingham, Trans. Faraday Soc., 67 (1971) 794.
2 E. Ma, Bull. Chem. Soc. Jpn., 37 (1964) 171.
3 M. Taniguchi and T. R. Ingraham, Can. J. Chem., 42 (1964) 2467.
4 I. B. Sharma and S. Batra, J. Thermal Anal., 34 (1988) 1273.
5 L. P. Domingues, R. L. Wilfong and L. R. Furlong, U.S. Bur. Mines, Report No. 6029 (1962) 19.
6 N. N. Greenwood and A. Earnshaw,Chemistry of the Elements, Pergamon, Oxford 1986, p. 1441.
7 X-ray Diffraction Data Card No. 4-0593, Powder Diffraction File, International Centre for Diffraction Data, Pennsylvania 1979.
8 P. Peyser and W. D. Bascom, in Analytical Calorimetry, Vol. 3, Eds. R. S. Porter and J. F. Johnson, Plenum, New York 1974, p. 537.
9 M. R. Udupa, Thermochim. Acta, 57 (1982) 377.
10 W. W. Wendlandt, J. Inorg. Nucl. Chem., 5 (1957) 118.
11 K. J. Laidler, Chemical Kinetics, Tata-McGraw-Hill, New Delhi 1983, p. 147.
12 A. M. Ginstling and B. I. Brounshtein, J. Appl. Chem. USSR, (English Tr.) 50 (1967) 484.
13 K. L. Mampel, Z. Phys. Chem., A187 (1940) 232; D. A. Young, Decomposition of Solids, Pergamon, Oxford 1966, p. 28.

Zusammenfassung — Mittels DSC und TG wurde die thermische Zersetzung von Ammoniumzersulfat untersucht. Die Ergebnisse zeigen in Sauerstoff einen fünfstufigen Zersetzungsprozeß im Temperaturbereich 364–1116 K. Ausgehend von den thermoanalytischen Angaben, der Elementaranalyse und den Messungen der magnetischen Suszeptibilität wurde eine Sequenz für die Zersetzung erstellt. Das Endprodukt wurde mittels Röntgendiffraktion als CeO_2 identifiziert. Ammoniumzersulfat und die Produkte des ersten und des letzten Überganges enthalten Zerionen mit der Oxydationsstufe +4, während in den drei Zwischenschritten Zerionen mit der

Oxydationsstufe +3 vorkommen. Anhand der nichtisothermen DSC-Untersuchungen wurden die kinetischen Parameter berechnet. Die isothermen Angaben zeigen, daß der Dehydratationsprozeß einem Ginstling-Brounstein Mechanismus folgt, während die folgenden drei Schritte durch das Mampelsche unimolekulare Gesetz der Randomkeimbildung bestimmt werden.